

# A Causal Model for Linear RF Systems Developed From Frequency-Domain Measured Data

Marissa Condon, *Member, IEEE*, Rossen Ivanov, and Conor Brennan, *Member, IEEE*

**Abstract**—With the ever-growing complexity of interconnect networks, models developed from measured data or data from 3-D electromagnetic simulators are increasingly becoming essential. It is to this end that the current contribution is directed. In particular, it focuses on the development of a model via a Fourier series expansion (FSE) approach. Its primary advantage is that the response in the time domain can be explicitly obtained in a simple form for an arbitrary input using only a set of FSE coefficients. Also, it guarantees causality without requiring a numerical implementation of a Hilbert transform. The end result is a causal and stable time-domain representation of a system that may subsequently be used in a time-domain simulator such as SPICE.

**Index Terms**—Fourier series expansion (FSE), high-speed interconnect, time-domain simulation.

## I. INTRODUCTION

WITH THE RAPID development in very large-scale integration (VLSI) technology, a variety of models have been proposed to accurately include the effect of complex interconnect networks in circuit design and analysis (e.g., see the review [1] and the extensive list of references therein). Furthermore, with the growing complexity of the geometry of modern interconnect networks, models developed from measured terminal data or full-wave electromagnetic (EM) simulations are required. Since interconnect behavior is best characterized in the frequency domain, these modeling techniques and methodologies involve the conversion of measured frequency-domain data to the time domain [2]. This enables their subsequent use in time-domain circuit simulators such as SPICE that are necessary for modeling complete nonlinear networks and systems. The methods for conversion of the data from the frequency domain to the time domain range from direct/inverse fast Fourier transform (FFT) to rational function approximations with subsequent partial fraction expansion to enable recursive convolution in the time domain ([3]–[11] and many others). The drawback with the rational function expansion approach is that the order of the numerator and denominator polynomials may be quite high. This incurs the usual numerical instability issues and problems of poor scaling although several approaches to overcome these difficulties have been suggested [3]–[7]. Another approach [8] based on resonant modeling of interconnects has been seen to

be very effective for small-scale networks. However, it does not explicitly address the issue of causality. One effective solution to the question of guaranteeing causality of the response of the network is that given by Perry and Brazil in [11] which uses an FFT-based Hilbert transform.

In the present paper, another solution is proposed that involves a frequency-domain based Fourier Series expansion (FSE) approach and obviates the need for an FFT. It automatically deals with or encompasses the causality issue. The proposed approach is effective for large-scale interconnect networks of arbitrary geometry described solely by frequency-domain network terminal measurements.

## II. MODEL

Consider a linear system described by a transfer function  $H(\omega)$ . Suppose  $H(\omega)$  is nonzero for  $|\omega| \in [0, \omega_m]$  where  $\omega_m$  is assumed to be large, but finite. It is assumed that  $H(\omega)$  is zero outside this interval. This assumption is valid for most realistic systems provided  $\omega_m$  is chosen large enough. Furthermore, assume Hermitian symmetry:  $H(\omega) = H^*(-\omega)$ . Then,  $\text{Re}H(\omega)$  may be expanded in a Fourier series as follows bearing in mind that it must be an even function of frequency

$$\text{Re}H(\omega) = \sum_{k=0}^{\infty} a_k \cos k\tilde{\omega} \quad (1)$$

where  $\tilde{\omega} = \pi\omega/\omega_m$ . The expression in (1) describes an even function, defined for  $\omega \in [-\omega_m, \omega_m]$  (i.e.,  $\tilde{\omega} \in [-\pi, \pi]$ ). Assuming causality, the expression for  $\text{Im}H(\omega)$  may be obtained from (1) via the Kramers–Kronig relations (Hilbert transform) [12], [13]

$$\text{Im}H(\omega) = -\sum_{k=0}^{\infty} a_k \sin k\tilde{\omega}. \quad (2)$$

Even if  $\text{Im}H(\omega)$  is available, causality should be checked and enforced if necessary. Noise and systematic errors can result in measured data that does not obey the Kramers–Kronig relations as discussed in [11].

From (1) and (2) it follows that

$$H(\omega) = \sum_{k=0}^{\infty} a_k e^{-jk\tilde{\omega}} \quad (3)$$

for  $\omega \in [-\omega_m, \omega_m]$ . Note that the Hermitian symmetry enforces some limitations on the transfer function: the coefficients  $\{a_k\}$  are real, and also, if  $H(\omega)$  has a complex pole, then its complex conjugate is also a pole. When dealing with the phase and magnitude representation, the system must be a minimum phase system (i.e.,  $H(\omega) \neq 0$  for  $\text{Im}(\omega) \leq 0$ ), otherwise

Manuscript received November 24, 2004. This paper was recommended by Associate Editor S. L. Netto.

M. Condon and C. Brennan are with the School of Electronic Engineering, Dublin City University, Dublin 9, Ireland (e-mail: marissa.condon@dcu.ie).

R. Ivanov is with the School of Electronic Engineering, Dublin City University, Dublin 9, Ireland. He is on leave from the Institute for Nuclear Research and Nuclear Energy, 1784 Sofia, Bulgaria.

Digital Object Identifier 10.1109/TCSII.2005.849019

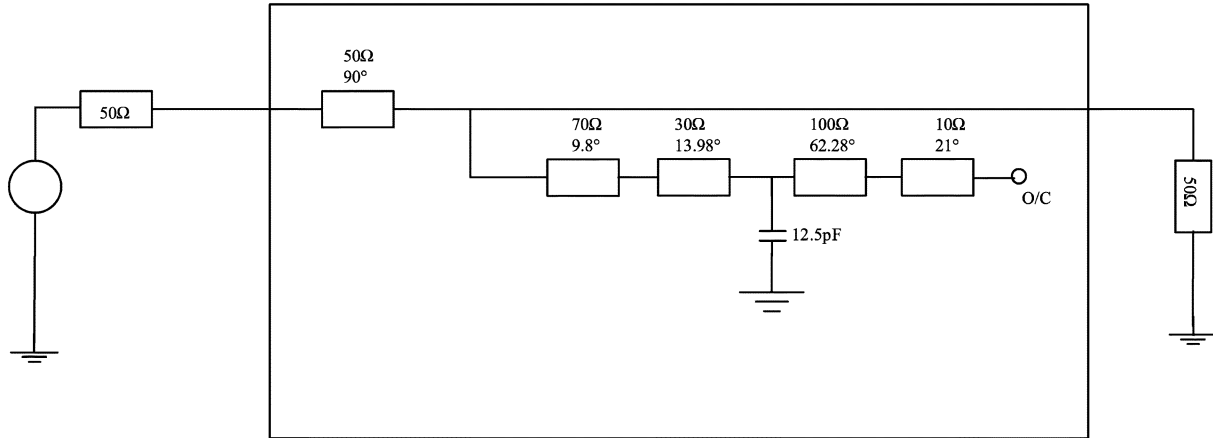


Fig. 1. Sample interconnect network.

$\log[H(\omega)]$  is not an analytic function for  $\text{Im}(\omega) \leq 0$ , even if  $H(\omega)$  is analytic.

The representation of the output in the time-domain may be obtained by an Inverse Fourier Transform. The output caused by an (arbitrary) input  $x(t)$  defined for  $t > 0$ , (i.e., input signal  $x(t)\theta(t)$  with Fourier image  $X(\omega)$  where  $\theta(t)$  is the unit step-function), due to (3) is

$$\begin{aligned} y(t) &= \frac{1}{2\pi} \int_{-\infty}^{\infty} e^{j\omega t} Y(\omega) d\omega \\ &= \frac{1}{2\pi} \int_{-\infty}^{\infty} e^{j\omega t} H(\omega) X(\omega) d\omega \\ &= \sum_{k=0}^{\infty} a_k \frac{1}{2\pi} \int_{-\infty}^{\infty} e^{j(t-\tilde{k})\omega} X(\omega) d\omega \\ &= \sum_{k=0}^{\infty} a_k x(t - \tilde{k})\theta(t - \tilde{k}) \end{aligned} \quad (4)$$

where  $\tilde{k} = \pi k / \omega_m$ .

Therefore, once the set of FSE coefficients  $\{a_k\}$  is obtained from the frequency-domain measurements (i.e., from (1)), then the response for an arbitrary input may be readily determined from (4). Furthermore, from (4), the coefficients  $\{a_k\}$  may be interpreted in the time-domain as giving the contribution of the input signal at a given time, preceding the output, to the output signal.

### III. IMPLEMENTATION

The central task in the proposed technique is the determination of the set of FSE coefficients  $\{a_k\}$ . While, in principle, an infinite number of coefficients is involved - in practice, only a finite number,  $N$ , of terms in (1) and (2) are used.

Suppose that the real or imaginary part (or both) of  $H(\omega)$  are measured at a number of points,  $\omega_i$ —i.e., suppose that the following data is known from measurements

$$F_i^{(1)} = \text{Re}H(\omega_i), \quad i = 1, 2, \dots, N_1 \quad (5)$$

$$F_i^{(2)} = \text{Im}H(\omega_i), \quad i = 1, 2, \dots, N_2 \quad (6)$$

where  $N_1$  is the number of measurements of the real part and  $N_2$  is the number of measurements of the imaginary part (the frequency sampling does not need to be uniform).

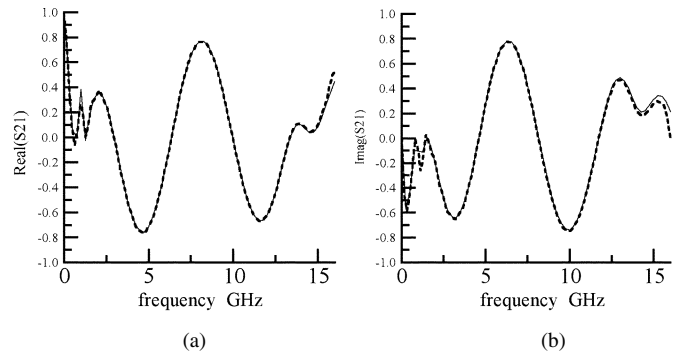
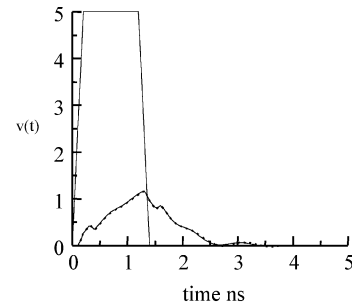
Fig. 2. (a) Real and (b) Imaginary parts of  $S_{21}$ .

Fig. 3. Transient results.

Then, let  $a$  be the set of real coefficients

$$a = [a_0 \quad a_1 \quad \dots \quad a_N]^t.$$

Let  $M_{ik}^{(1)} = \cos k\tilde{\omega}_i$ ,  $M_{ik}^{(2)} = -\sin k\tilde{\omega}_i$  and  $\tilde{\omega}_i = \pi\omega_i/\omega_m$  where  $k = 1, \dots, N$ .

Then, from (1) and (2)

$$F^{(1)} = M^{(1)}a + E^{(1)} \quad (7)$$

$$F^{(2)} = M^{(2)}a + E^{(2)}. \quad (8)$$

$E^{(1,2)}$  represent the errors that arise due to limiting the summation in (1)–(4) to a finite number of terms,  $N$ . Note that (7) represents a formulation for the least-squares method and therefore provides the best approximation for  $a$  by minimizing the error  $E^{(1)T}E^{(1)}$ .

$$a = (M^{(1)T}M^{(1)})^{-1}. \quad (9)$$

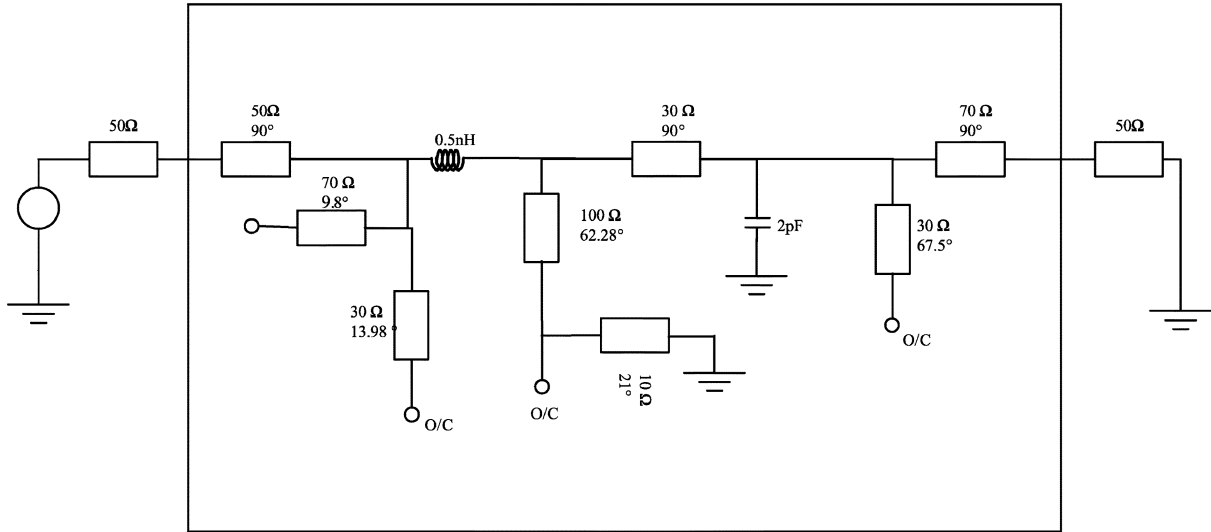


Fig. 4. Second sample interconnect network.

The system in (8) may be used to retrieve all the elements of  $a$  with the exception of  $a_0$  since  $M_{i0}^{(2)} \equiv 0$ . However, if data for both the real and the imaginary parts is available, then (7) and (8) may be merged to yield

$$F = Ma + E \quad (10)$$

with

$$F = \begin{bmatrix} F^{(1)} \\ F^{(2)} \end{bmatrix} \quad M = \begin{bmatrix} M^{(1)} \\ M^{(2)} \end{bmatrix} \quad E = \begin{bmatrix} E^{(1)} \\ E^{(2)} \end{bmatrix}$$

and the minimal error  $E^T E$ , for (10) is achieved with

$$a = (M^T M)^{-1} M^T F. \quad (11)$$

In order to apply the least-squares method with (11) it is essential that

$$N < \dim(F) = N_1 + N_2.$$

(When (9) is employed,  $N < \dim(F) = N_1$ ).

Thus, the more measurement data that is available, then more coefficients  $\{a_k\}$  may be found and consequently, a better resultant interpolation of (1) may be achieved.

Once the vector of coefficients  $a$  is found from either (9) or (11), the response of the system for an arbitrary input from (4) is

$$y(t) = \sum_{k=0}^N a_k x \left( t - \frac{k\pi}{\omega_m} \right) \theta \left( t - \frac{k\pi}{\omega_m} \right). \quad (12)$$

The precision of (12) clearly increases with increasing  $N$ . Thus, the accuracy of the method is only limited by the volume of the available measurement data. Also, in order to represent the output on the time interval  $[0, T]$  the number of FSE coefficients needed is

$$N \geq \omega_m T / \pi.$$

Note that the FSE coefficients (vector  $a$ ) are obtained from the measurement data (vector  $F$ ) through a simple linear transformation (11)! Furthermore, because of the use of a Fourier Series

as opposed to a polynomial based approach, the problems with ill-conditioning do not arise. Note also that (12) enables the reverse problem to be solved- if the input and output are known in the time domain, then the FSE coefficients, and consequently, the transfer function may be recovered from (3).

#### IV. NUMERICAL EXAMPLES

The first example chosen is the lossy interconnect network shown in Fig. 1. Measurements of the scattering parameters at 65 frequencies are available. Fig. 2 shows the measured and simulated (with new approach) scattering parameter,  $S_{21}$ . The real and imaginary parts are shown. In all results, the dashed line corresponds to the simulated result and the solid line corresponds to the measured result. Note that the measured results are for frequencies up to 16 GHz and at that frequency  $S_{21}$  does not tend to zero. It is assumed that  $S_{21}$  is zero (both the real and imaginary parts) for all frequencies, higher than 16 GHz. This assumption, strictly speaking, violates the causality, and is the reason why there is a small discrepancy between the measured and simulated result around 16 GHz, since the approximation is always causal by construction. For all other frequencies however there is a very good agreement. Fig. 3 shows the transient output response for a 5-V pulse input with a rise and fall time of 200 ps and a duration of 1.4 ns.

The second example chosen is that of the network shown in Fig. 4. Fig. 5 shows the measured and simulated results for the scattering parameter  $S_{21}$  as an example (All scattering parameters are equally well approximated). Fig. 6 shows the measured and simulated transient result for a trapezoidal input with amplitude = 5 V, rise - /fall - time = 200 ps and a total duration = 1.4 ns. As evidenced again from the results, the method is highly effective. Furthermore, it has the advantage that causality is automatic and that no FFT algorithm is required. A simple linear transform (11) as required from the least-squares method is all that is needed. It should be noted that the technique is independent of the complexity of the network topology. All that is required is a set of measured scattering parameters. It is also independent of the input signal.

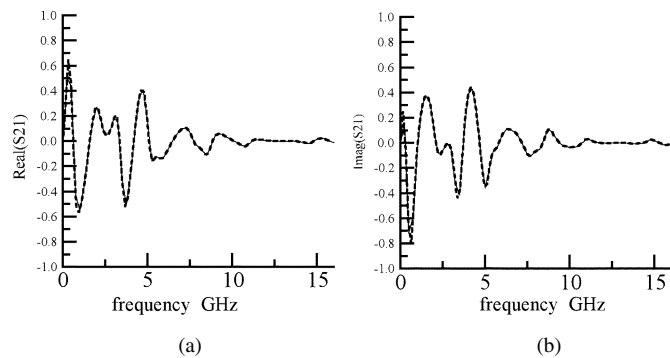


Fig. 5. (a) Real and (b) imaginary parts of  $S_{21}$ .

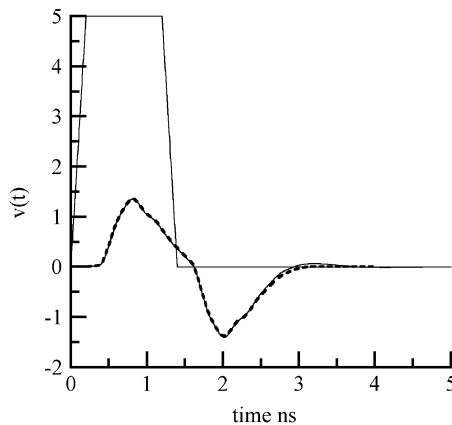


Fig. 6. Transient results.

TABLE I  
VARIATION OF APPROXIMATION ERROR WITH NUMBER OF FOURIER  
COEFFICIENTS TAKEN

Number of the coefficients used; $N$	Error, $E^T E$ (Example-Fig.1)	Error, $E^T E$ (Example-Fig.4)
10	1.74	4.29
20	0.66	1.50
30	0.39	0.62
40	0.15	0.22
50	0.14	0.02
60	0.13	0.004

The approximation error decreases with the number  $N$  of the Fourier coefficients taken, as it is shown at Table I. In both examples 65 experimental points are used for the computation of the Fourier coefficients.

## V. CONCLUSION

A frequency-domain FSE Approach for determining transient responses from measured scattering parameters is given. The method is advantageous in that it obviates the need for an FFT-based Hilbert transform or chirp z-transform to guarantee causality. It is very straightforward to implement.

The method obviously has a general applicability in any situation involving conversion between the frequency-domain and the time domain. The technique is particularly convenient for system identification (of a “black-box” system), when a large amount of frequency-response experimental data is available.

## ACKNOWLEDGMENT

The authors wish to thank Prof. Brazil and the Microwave Research Unit, University College Dublin, Dublin, Ireland, for the provision of the measured results.

## REFERENCES

- [1] R. Achar and M. Nakhla, “Simulation of high-speed interconnects,” *Proc. IEEE*, vol. 89, no. 5, pp. 693–728, May 2001.
- [2] B. Ulriksson, “Conversion of frequency-domain data to time-domain,” *Proc. IEEE*, vol. 74, no. 1, pp. 74–77, Jan. 1986.
- [3] W. T. Beyene and J. E. Schutt-Ainé, “Accurate frequency-domain modeling and efficient circuit simulation of high-speed packaging interconnects,” *IEEE Trans. Microw. Theory Tech.*, vol. 45, no. 10, pp. 1941–1947, Oct. 1997.
- [4] —, “Efficient transient simulation of high-speed interconnects characterized by sampled data,” *IEEE Trans. Compon. Packag. Manuf. Technol. B*, vol. 21, no. 1, pp. 105–114, Feb. 1998.
- [5] W. T. Beyene, “Improving time-domain measurements with a network analyzer using a robust rational interpolation technique,” *IEEE Trans. Microw. Theory Tech.*, vol. 49, no. 3, Mar., 2001.
- [6] M. Elzinga *et al.*, “Pole-residue formulation for transient simulation of high-frequency interconnects using householder LS curve-fitting techniques,” *IEEE Trans. Compon. Packag. Manuf. Technol. B*, vol. 23, no. 2, pp. 142–147, May 2000.
- [7] Z. Marićević, T. K. Sarkar, Y. Hua, and A. R. Djordjević, “Time-domain measurements with Hewlett-Packard network analyzer HP 8510 using the matrix pencil method,” *IEEE Trans. Microw. Theory Tech.*, vol. 39, no. 3, pp. 538–547, Mar. 1991.
- [8] M. Condon and E. Dautbegovic, “Efficient modeling of interconnects in high-speed circuits,” in *Proc. Eur. Conf. Circuit Theory and Design*, Krakow, Poland, 2003.
- [9] T. Brazil, “Causal-convolution—A new method for the transient analysis of linear systems at microwave frequencies,” *IEEE Trans. Microw. Theory Tech.*, vol. 43, no. 2, pp. 315–323, Feb. 1995.
- [10] P. Perry and T. Brazil, “Hilbert-transform-derived relative group delay,” *IEEE Trans. Microw. Theory Tech.*, vol. 45, no. 8, pp. 1214–1225, Aug. 1997.
- [11] —, “Forcing causality on S-parameter data using the Hilbert transform,” *IEEE Microw. Guided Wave Lett.*, vol. 8, no. 11, pp. 378–380, Nov. 1998.
- [12] J. D. Jackson, *Classical Electrodynamics*, 2nd ed. New York: Wiley, 1975.
- [13] J. G. McDaniel, “Applications of the causality condition to acoustic reflections,” in *Proc. 1997 ASME Design Engineering Technical Conf.*, Sacramento, CA, Sep. 14–17, 1997.